International Journal of Mechanical Engineering and Robotics Research

ISSN 2278 – 0149 www.ijmerr.com
Vol. 2, No. 4, October 2013

Research Paper

THE EFFECT OF SHIELDING GASES ON MECHANICAL PROPERTIES AND MICROSTRUCTURE OF AUSTENITIC STAINLESS STEEL WELDMENTS

N R Anand[1], Vijaysingh M Chavan[1]* and Nitin K Sawant[1]

*Corresponding Author: Vijaysingh M Chavan, ✉ vijaysingh_chavan@yahoo.co.in

In this study AISI 304 L type of austenitic stainless steels were welded using 308 L consumable electrodes by the process of Gas Metal Arc Welding (GMAW). The aim of current study is to examine effects of shielding gas compositions on mechanical properties and microstructure of AISI 304 L weldments. A detailed study of gas metal arc welding of AISI 304 L stainless steel was carried out with different shielding gas compositions such as 100% argon, 80% argon + 20% CO_2, 50% Argon + 50% argon and 100% CO_2. The mechanical properties were determined by performing different tests, viz. Charpy V notch impact test, tensile test, hardness test, bend test. Surface morphology had been analyzed by Scanning Electron Microscope (SEM). The results indicated that the shielding gas compositions have great influence on mechanical properties. Results revealed that increase in amount of CO_2 in shielding gas resulted in higher tensile strength and hardness values than the base metal. The study also indicated that shielding gas composition also have an influence on toughness values which further depends upon ¢-ferrite content in the weld metal. This ¢-ferrite content decreases with increase in CO_2 percentage of shielding gases. Decrease in ¢-ferrite content has negative effects on toughness values of weldments. The gas metal arc welding is found to be suitable for welding of AISI 304 L austenitic stainless steels owing to their high welding speed and excellent mechanical properties.

Keywords: Shielding gases, Austenitic stainless steel 304 L, GMAW, Mechanical properties

INTRODUCTION

Throughout several years, Austenitic Stainless Steels (ASS) have been employed in industrial applications that range from pipes and pressure vessels to structural purposes. The influences that these materials have on the industry are mainly due to their mechanical strength as well as their excellent corrosion

[1] Department of Mechanical Engineering, College of Engineering, Pune, India.

resistance, which can also be attributed to the austenitic phase that appear in the matrix of the material when alloying elements like nickel, manganese, and nitrogen are combined at high quantities. Similarly, several methods of joining, like welding, have been broadly performed for these metals because of the low price and high quality of this process. Additionally, for the industrial applications of the AISI/SAE 304 stainless steels, the welding method is widely used due to its simple assembly and which joins sheets, plates and pipes made up of this material. On the other hand, it is also imperative to highlight that during welding many discontinuities are produced, which acts as stress raisers that can lead to a decrease in the life of the weld. Therefore, the problems of this joining method have become an important issue of study in manufacturing. The austenitic stainless steels (Fe-Cr-Ni) have excellent mechanical properties and corrosion resistance. Due to having combine properties, their usage in various applications such as storage tanks, pipe, and pressures vessel valves, pumps, distiller etc have been increasing. Better strength, toughness and formability are required for this kind of applications mentioned above (Kou, 2003). 300 series austenitic stainless steels are most popular steels and their most important and conspicuous properties are their excellent toughness and corrosion resistance (Liao and Chen, 1998; Budinski and Budinski, 1999; Kou, 2003; and Shigley, 2004). Due to fcc structure of austenitic stainless steels, they have higher toughness values which is almost independent of temperature, thus brittle failure does not occur like low carbon steels which have bcc structure. Austenitic stainless steels maintain their higher notch toughness even at cryogenic temperature. The mechanical properties of austenitic stainless steels provide an excellent combination of better strength, ductility and toughness over a broad temperature range (Liao and Chen, 1998; and Liao and ve Chen, 1999). The selection of the shielding gas is crucial for obtaining optimal properties of the weldments. Therefore, number investigations have been performed to study the effect of shielding gas composition on mechanical properties of austenitic stainless steel weldments. Determination of mechanical properties such as hardness, impact toughness and tensile strength, etc., of the component made from austenitic stainless steel weldments is crucial for its safe use. Those constructions can be exposed dynamic load during working in various applications, therefore, impact toughness behavior become more important under different working condition such as temperature and environment.

The present study investigates the influence of shielding gas composition on the notch impact toughness of AISI 304 L austenitic stainless steels. Four different gas compositions were used for the purpose of shielding. Optical and scanning electron microscopy studies and hardness measurement were also carried out so as to analyze effect of shielding gases.

EXPERIMENTAL PROCEDURE

AISI 304 L grade austenitic stainless steel plates of dimensions (125 mm x 250 mm x 8 mm) were used in this study. Austenitic stainless steel grade 308 L wire with diameter of 1.2 mm was used as consumable electrode.

The chemical compositions of base material and filler material are given in Table 1.

Table 1: Chemical Composition of Base and Filler Material Used

Elements	Base Material 304L Wt (%)	Consumable 308 L Wt (%)
C	0.0220	0.028
Mn	1.7200	1.650
Si	0.3600	0.430
S	0.0084	0.020
P	0.0250	0.021
Cr	18.1300	19.700
Ni	8.4400	9.300
Cr Eq.	20.1400	21.830
Ni Eq.	12.5900	14.140

Figure 1: Edge Preparation for Weld Joint

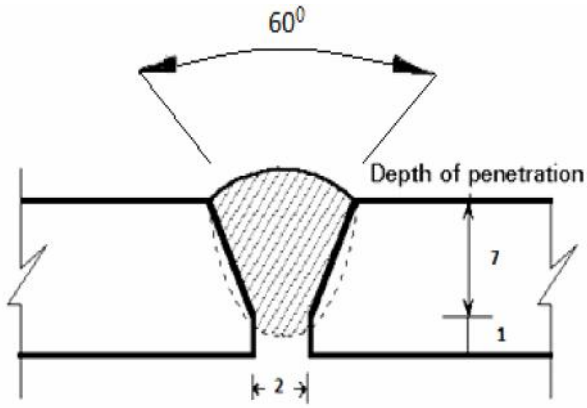

The austenitic stainless steel 304 L plates were prepared for welding by GMAW with the dimensions 250 mm (l) x 150 mm (w) x 8 mm (t). Butt joint configuration was used. Before this V shaped edges were prepared with 600 included angles between two edges. Three different passes of GMAW were performed. Welding process was carried out using different shielding gas compositions such as 100% argon, 80% argon + 20% CO_2, 50% argon + 50% CO_2 and 100% CO_2 with constant gas flow rate of 15 liters/min. Interpass temperature was kept below 150 °C due to lower thermal conductivity of austenitic stainless steels.

The welding parameters used were selected according to suggestions of product catalogue and experiences obtained earlier. The welding parameters are shown in Table 2.

Table 2: Welding Parameters

S. No.	Parameter	Value
1.	Welding Current (I)	200
2.	Voltage (V)	28
3.	Speed (mm/min)	120
4.	Heat Input (KJ/m)	2.8
5.	Gas Flow (Lit/min)	15

As seen from the table, welding current is kept 200 Ampere and voltage is 28 volt. Constant welding speed of 120 mm/min was maintained. This welding system provides the constant heat input of 2.8 KJ/m during welding processes.

The welded joints were sliced (as shown in Figure 2) using abrasive cutting and then machined to the required dimensions for preparing tensile, impact test, bend and metallographic specimens.

Figure 2: Extraction of Test Samples

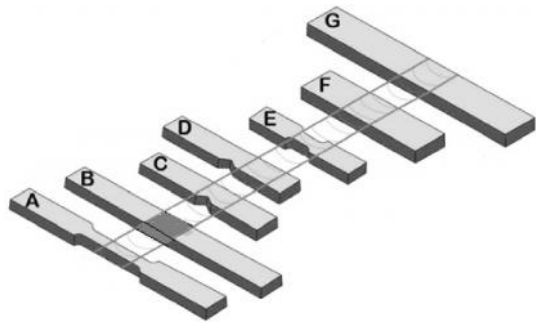

Microhardness measurements were carried out across the weld metal and base metal for which 1 Kg load was applied during measurements. Microstructure examination was carried out on cross section of the weldments. The specimens were mounted later flatted and then grounded using SiC abrasive paper with grit ranges from 180 to 1200. Then the samples were lightly polished using lapping machine. Samples were then washed, cleaned by alcohol and then dried, followed by electrolytic etching in 10% oxalic acid at 9 V for 30 s. Metallographic examination of samples were performed using scanning electron microscopy. Chemical composition of weld metal was determined by using Spectrometry. Ferrite numbers of the weld metal were measured theoretically and also by using ferrite-scope equipment.

RESULTS AND DISCUSSION

There were no any observations of spatters generated under all gas composition except little spatters generation using of 100% CO_2 shielding. This indicates that a stable arc is obtained under all the gas composition. Better weld bead appearance was obtained after GMAW process which points out that GMAW process provides better appearance and weld quality. As mentioned in earlier investigation by Liao and Chen (1998) and Liao and ve Chen (1999) the spatter rates increase with increasing CO_2 content in the shielding gas composition. Higher CO_2 content causes larger and numbers of spatter particles. This spatter rate is increased by oxygen potential of shielding gas. Of course, an increase of CO_2 content in the shielding gas naturally results in increasing oxygen potential of the gas. Welding current during GMAW process has higher values than that of FCAW process. The ferrite numbers in the weld metal were measured. The effect of CO_2 content in the shielding gas on ferrite content is pronounced. The ferrite content in the weld metal is decreased by increasing the amount of CO_2 in the shielding gas. Carbon is austenite stabilizing element and widens austenitic area in the weld metal (Kou, 2003). The increase of CO_2 content in the shielding gas resulted in increasing amount of carbon in the deposited metal. Thus the ferrite number decreases, which provides larger austenitic area in the weld metal due to increasing of Ni equivalent value. Higher percentage of CO_2 resulted in higher oxygen potential therefore, consumption of Cr and Si increase due to oxidation, which causes lowering of Cr equivalent value and narrowing ferrite area in the weld metal. The results obtained in this study are consistent with earlier literature (Liao and Chen, 1998; and Liao and ve Chen, 1999). The amount of delta-ferrite was estimated using Cr and Ni equivalent of the weld metal. Delta-ferrite is solidified firstly which decreases crack susceptibility during cooling. The percentage of ä-ferrite in the weld metal was determined with the help of WRC-1952 constitution diagram as function of Cr and Ni equivalent value. The other elements are also effective during cooling. According to earlier studies, about 3-4% volume ferrite prevents the weld metal from solidification cracking. Ferrite number of 4 is preferable for preventing hot cracking during the cooling of the weld metal. Sometimes, cracks may be seen in deep and narrow of weld metal during usage of the welding methods having higher heat input.

Weld Chemistry and Ferrite Content

Weld metal composition and ferrite content was determined for each sample. The measured chemical composition of the weld metal is listed in Table 3. It is observed that there is great influence of shielding gases on weld metal composition which further becomes responsible for ferrite content in weld metal. As seen from the table, carbon and nickel content in the weld metal increase with increase in the CO_2 content of the shielding gas. The weld chemistry plays important role in phase balance which further defines the mechanical properties.

Table 3: Chemical Composition and Cr and Ni Equivalents

Element	Weight Percentage (Argon + CO_2)			
	100% Argon	80% Argon	50% Argon	100% CO_2
C	0.0220	0.026	0.032	0.038
Mn	1.10	1.44	2.02	2.29
Mo	0.186	0.291	0.302	0.338
Nb	0.0105	0.0106	0.0128	0.0215
Si	0.289	0.628	0.388	0.318
N	0.058	0.113	0.116	0.121
Cu	0.430	0.439	0.376	0.368
S	0.006	0.007	0.007	<0.001
Cr	18.44	18.73	18.58	18.44
Ni	7.84	8.03	7.74	7.69
Cr Eq.	18.633	19.028	18.891	18.793
Ni Eq.	9.8775	11.3098	11.2740	11.5320

It is well known that nickel and carbon are strong austenite stabilizing elements. Therefore, the CO_2 increase in shielding gas resulted in decrease of Cr equivalent on the other hand, increasing of Ni equivalent. In addition to that, an increase of CO_2 percentage in the gas increases consumption of Cr, Si and Mn.

The amount of ¢-ferrite in the weld metal is calculated using the composition of base metal, filler metal as function of Cr equivalent and Ni equivalent for which WRC-92 constitution diagram was used. The calculation of ¢-ferrite ratio gives the values from 6% to 11% however, those are estimated values. Ferrite contents by using ferrite-scope apparatus was from 6 to 12. All the estimated and measured values of ferrite content are listed in Table 4.

Table 4: Average Ferrite Content

S. No.	Weld Samples with Shielding Gas	Ferrite Content (from Constitution Diagram)	Ferrite Content (by Ferrite-Scope)
1.	100% Argon	11	12
2.	80% Argon + 20% CO_2	8	9
3.	50% Argon + 50% CO_2	7	8
4.	100% CO_2	6	6

Microhardness Test Results

The microhardness (VHN) test was performed on the etched transverse cross-section of the weld zone using a load of 1 Kg, which was applied for duration of 15 sec. The mean value of three different measurements was taken as exact value for the hardness. It has been found that, weld metal shows highest hardness. HAZ shows intermediate hardness whereas base metal is having lowest hardness. Hardness values of all 304 L weldments taken in the centre of weld metal are higher than that of those taken in HAZ and base metal. It was found that the higher values were especially obtained nearer to surface, i.e., away from weld centerline. According to the previous studies,

the weld metal produced in multipass welding process was shown work hardened state with dislocation density exceeding as compared with the dislocation density of in fully annealed austenitic stainless steels. The increase in dislocation density is because of repeated thermal cycles experienced by the solidified metal during multipass welding (Shamsul and Hisyam, 2007).

C1 = 100% Argon shielding

C2 = 80% Argon + 20% CO_2 shielding

C3 = 50% Argon + 50% CO_2 shielding

C4 = 100% CO_2 shielding

Table 5: Microhardness Values Across Weld Joint

Distance from Weld Center (mm)	Microhardness VHN			
	C1	C2	C3	C4
–6	228.9	228.2	229.4	223.6
–5.5	229.2	224.6	227.8	225.2
–5	228.9	228.4	228.4	223.2
–4.5	229.2	229.5	226.8	228.6
–4	252.1	246.2	244.4	240.2
–3.5	252.2	248.2	246.5	242.6
–3	252.6	247.1	248.2	244.2
–2.5	254.4	248.9	246.4	244.8
–2	252.3	246.8	245.8	243.5
–1.5	272.8	265.9	262.7	258.2
–1	273.2	266.4	264.2	257.9
–0.5	274.1	266.6	264.4	258.4
0	275.9	269.2	267.8	258.8
0.5	274.4	267.4	265.2	257.2
1	276.2	267.0	266.8	259.2
1.5	274.2	267.8	264.2	257.8
2	274.1	269.2	267.3	258.6
2.5	273.9	268.2	267.9	257.8
3	252.8	246.8	245.9	243.8
3.5	253.2	247.2	244.7	243.4
4	254.4	248.4	244.3	244.8
4.5	254.8	249.2	246.1	244.4
5	255.2	246.2	248.7	244.9
5.5	228.2	228.9	227.8	228.8
6	229.0	226.8	228.2	226.4

Table 5 (Cont.)

Tensile Test Results

Tensile test results mainly showed that the fracture occurs away from the joint in each sample plate. Among the four shielded weld metals, tensile strength of weld metal is higher than the base material. In particular, for 100% CO_2 gas shielded weld test plate the value of tensile strength is highest, i.e., 594 MPa. The tensile strength of a test plate welded with shielding gas mixture of 80% Ar and 20% CO_2 is found to be intermediate and the magnitude of ultimate tensile strength was found to be 580 MPa. The tensile strength of weld sample with 50% argon and 50% CO_2 was found to be 588 MPa. Finally the value of ultimate tensile strength for weld with 100% argon as shielding gas was found to be 575 MPa.

Table 6: Tensile test Results

S. No.	Shielding Gas	Yield Strength (MPa)	Ultimate Tensile Strength (MPa)	Fracture Location
1.	100 % Argon	254	575	Base Metal
2.	80% Argon + 20% CO_2	282	580	Base Metal
3.	50% Argon + 50% CO_2	294	588	Base Metal
4.	100% CO_2	310	594	Base Metal
5.	Base Metal	234	585	Base Metal

Impact Test Results

The impact energies of the weldments by GMAW were given in Table 4, which show that impact energy decreases with decreasing ¢-ferrite containing in the weld metal. It is known that the austenite has FCC structure and delta ferrite a Body Centered Cubic (BCC) structure. FCC metal has a high notch toughness which is almost independent of temperature, thus brittle fracture does not occur. On the other hand, the notch toughness of BCC metal is strongly dependent on temperature; therefore, brittle fracture is severe at low temperature, while at higher temperature it shows ductile rupture. It is also obvious that notch toughness of all weld metal is affected by delta ferrite and oxygen potential and higher oxygen potential results in a degradation of notch toughness.

Table 7: Impact Strength of Weldments

S. No.	Shielding Gas	Impact Strength in Weld Metal (Joules)
1.	100% Argon	72
2.	80% Ar + 20% CO_2	62
3.	50% Ar + 50% CO_2	58
4.	100% CO_2	55

Bend Test Results

Bend tests (root bend test and face bend test) were carried out on sample piece of each test plate. It is found that sample has not braked at the weld line even there were no signs of cracking at the weld interface. The strip has shown even radius without any sharp angle change. Thus, both bend tests showed satisfactory results.

Salt Spray test Results

The salt spray corrosion test was carried out using standard test method IS 9000/1983. Salt spray test was carried out using 5% NaCl solution with pH about 6.8. The results of salt spray corrosion test were found satisfactory. After each interval of 24 hours, samples were inspected for four successive days. After 24, 48, 72, 96 hours any white or red colored rust is not observed, thus this test also concluded satisfactory results for all four samples of 304 L stainless steel welds.

Metallographic Results

Scanning electrode microscopy studies were shown in Figures 3-6. These micrographs were taken from the weld metals. The microstructure of weld metal and ä-ferrite ratio can be assessed using one of the Schaeffler, De-Long and WRC diagrams. The latest WRC constitution diagram is used for present study with consideration of chemical composition of base metal and filler materials after welding. Owing to non-equilibrium rapid solidification condition in welding process, peak temperature in fusion zone is much higher than the upper limit of phase balance between ¢-Fe and ¥-Fe phase. The austenite starts to precipitate at the grain boundaries of ferrite during the cooling. Since the ¢-¥ transformation is diffusion controlled process, because of faster cooling in welding process there is lack of sufficient time for completion of transformation. As a result a large portion of primary ¢-Fe is retained in joints. Typical microstructures of fusion zone and weld metal are shown in figures. Almost all joints composed of dark ¢-ferrite dendritic structure in matrix of austenite. However, different grain sizes can be observed in all the joints. Obviously, maximum ferrite number of 11 was observed by using constitution diagrams for the weld sample welded with 100% argon

Figure 3: 100% Argon Shielding Weld

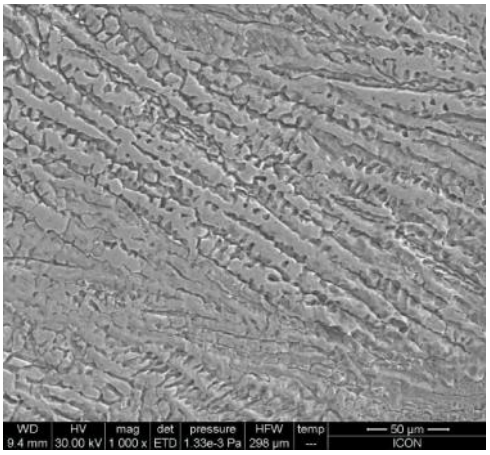

Figure 4: SEM of Weld Metal Shielded with 80% Ar + 20% CO_2

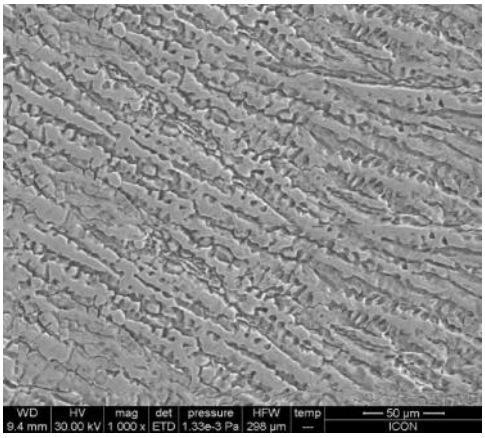

Figure 5: SEM of Weld Metal Shielded with 50% Ar + 50% CO_2

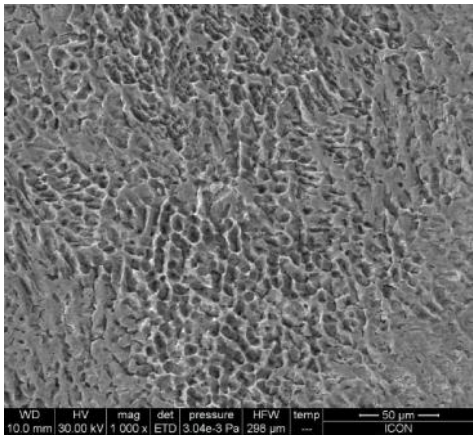

Figure 6: SEM of Weld Metal Shielded with 100% CO_2

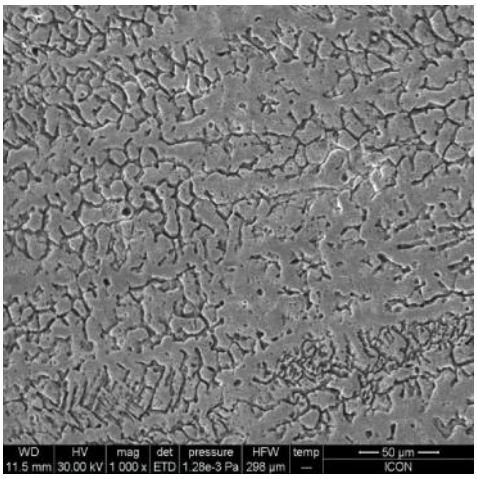

shielding. This highest ferrite content was confirmed by using ferrite-scope measurement technique. Ferrite-scope indicated ferrite number 12 for this weld joint. For weld samples welded using 80% argon and 50% argon, ferrite number was 8 and 7 respectively by using constitution diagram. Ferrite-scope indicated ferrite number of 9 and 8 respectively for these samples. These values of ferrite number were found intermediate between those values of argon shielded and CO_2 shielded samples. Minimum ferrite number was observed for weld sample welded using 100% CO_2 shielding using constitution diagram which was around 6. This lowest value of ferrite number was confirmed by using ferrite-scope. Ferrite-scope indicated ferrite number of 6 for the sample welded with 100% CO_2 shielding. These micrographs were taken from both fusion zone and the weld metals. It is clearly seen that ¢-ferrite content decreases with the increasing of CO_2 content in the shielding gas from calculated values of Nickel and Chromium equivalents. These

¢-ferrite numbers for 304 L welds 100% CO_2 and 100% argon shielding were determined as 6 to 11 respectively using constitution diagram. Owing to the non-equilibrium rapid solidification condition in welding process, the peak temperature in fusion zone is much higher than the upper limit of phase balance between ¢-Fe and ¥-Fe phase. The austenite starts to precipitate at the ferrite grain boundaries during the cooling of joints in the higher temperature range 1573-1073 K. Since the ¢- ¥ transformation is a diffusion-controlled process, the fast cooling in the welding process does not offer sufficient time to complete the phase transformation. As a result, a large portion of primary ¢-Fe is retained in joints. Furthermore, the incomplete transformation results in the retention ¢-ferrite.

It is thought that impact energy values are connected with delta-ferrite content in the weld metal. Higher delta-ferrite percentages increase the strength of the weldment. Therefore, it also increases the impact energy values. It is well known that the impact energy values obtained at lower temperatures are less than the values of obtained at higher temperatures. It is also known that austenite has FCC structure and delta-ferrite has BCC structures. FCC structure has higher toughness values and temperature independence. On the other hand, BCC structure has lower toughness and strongly temperature dependence. Impurities occurred in the microstructure due to increasing CO_2 percentages in the shielding gas may be resulted in reduction of the toughness values. If certain ratio of the ferrite exists between dendrites in the solution, brittle phases that can be occurred will be arrested in the ferrite. In addition to that deformation ability of ferrite is much better than that of austenite. The existence a few percent of ferrite is useful to remove the tensile stress. Thus, risk of microcraking during the solidification is also prevented. As the weld pool cooled rapidly after welding and extremely high solidification growth rate occurred. No evidence of microcraking was encountered during microstructure investigation. Estimated ferrite content and overall phase balance can be correlated to mechanical properties. For weld samples welded with mixtures of argon and hydrogen shielding, impact test results are tabulated in table. Maximum impact energy of 72 joules was absorbed for weld specimen welded with 100% argon shielding, whereas minimum impact energy of 55 joules was absorbed for weld specimen welded with 100% CO_2 shielding. This change in impact toughness values can be attributed to existence of ferrite content in weld joints.

It is thought that impact energy values are connected with ¢-ferrite content in the weld metal. Higher ¢-ferrite percentages increase the strength of the weldment. Therefore, it is also increases the impact energy values. It is also thought that the impact energy values obtained at 0 °C are always less than the values of obtained at higher temperatures. It is known that the á ferrite has a fcc structure and ¢-ferrite has bcc structures. fcc structure has higher toughness values and temperature independence (Dieter, 1988; Liao and ve Chen, 1999; Ghosh *et al.*, 2009; and Shamsul, and Hisyam, 2007). Impact energy was decreased by increasing oxygen potential in shielding gas. At lower temperature such as 0 °C delta ferrite shows brittle nature.

CONCLUSION

In this study, AISI 304 L austenitic stainless steels were welded by GMAW. The following conclusions can be drawn from the experimental results:

- AISI 304L austenitic stainless steels were welded by GMAW using various gas composition. Any spatter problems were not observed during the welding process.
- Carbon percentage in the weld metal increases with increasing of CO_2 content of the shielding gas, which causes a decrease of ferrite amount and an increase in austenite area.
- Usage of various gas compositions during GMAW process resulted in difference in hardness values of the weld metals. It is attributed to percentage of carbon and ferrite content in the weld metal.
- Spectroscopy analysis shows that difference in gas composition have a great influence on changing chemical composition of the weld metal. Some elements such as Cr, Si and Mn may be decreased depending on CO_2 content in the gas composition due to oxidation of those elements.
- In the microstructure investigation, the existence of some ¢-ferrite in the weld metal was confirmed. ¢-ferrite percent determined using WRC diagrams, which varied between the values of 6% and 11%. In addition, microstructure of the weld metal shows mixture of austenite and ferrite.
- The study also showed that variation of toughness values depended on ¢-ferrite content in the weld metal. ¢-ferrite content decrease with increasing CO_2 percentages in the shielding gas. The impact energies are decreased with increasing CO_2 content in the shielding gas. Thus, decreasing ¢-ferrite rate in the weld metal have negative effects on the toughness values of the weldments.

REFERENCES

1. Budinski K G and Budinski M K (1999), *Stainless Steels, Engineering Material*, 6th Edition, pp. 455-461.
2. Dieter G E (1988), *Mechanical Metallurgy*,p. 476, McGraw-Hill, London.
3. Ghosh P, Dorn L, Kulkarni S and Hofmann F (2009), "Arc Characteristics and Behaviour of Metal Transfer in GMA Welding of Stainless Steel", *Journal of Materials Processing Technology*, p. 209.
4. Kou S (2003), *Welding Metallurgy*, Ajohn Wiley & Sons Publications.
5. Liao M T and Chen P Y (1998), "The Effect of Shielding-Gas Compositions on the Microstructure and Mechanical Properties of Stainless Steel Weldments", *Materials Chemistry and Physics*, Vol. 55, pp. 145-151.
6. Liao M T and ve Chen W J (1999), "A Comparison of Gas Metal Arc Welding with Flux-Cored Wires and Solid Wires Using Shielding Gas", *The International Journal of Advanced Manufacturing Technology*, pp. 49-53.
7. Shamsul J and Hisyam M (2007), "Study of Spot Welding of Stainless Steel Type 304", *Journal of Applied Science Research*, Vol. 3, No. 11, pp. 1494-1499.
8. Shigley M (2004), *Mechanical Engineering Design*, 7th Edition, McGraw Hill.